

Turbulence velocimetry of density fluctuation imaging data

G. R. McKee,^{a)} R. J. Fonck, D. K. Gupta, D. J. Schlossberg, and M. W. Shafer
University of Wisconsin—Madison, 1500 Engineering Drive, Madison, Wisconsin 53706 USA

C. Holland and G. Tynan
University of California, San Diego, 9500 Gilman Drive, La Jolla, California 92037 USA

(Presented on 19 April 2004; published 4 October 2004)

Analysis techniques to measure the time-resolved flow field of turbulence are developed and applied to images of density fluctuations obtained with the beam emission spectroscopy diagnostic system on the DIII-D tokamak. Velocimetry applications include measurement of turbulent particle flux, zonal flows, and the Reynolds stress. The flow field of turbulent eddies exhibits quasisteady poloidal flows as well as high-frequency radial and poloidal motion associated with electrostatic potential fluctuations and strongly nonlinear multifield interactions. The orthogonal dynamic programming technique, developed for fluid-based particle and amorphous shape (smoke) flow analysis, is investigated to measure such turbulence flows. Sensitivity and accuracy are assessed and sample results discussed. © 2004 American Institute of Physics. [DOI: 10.1063/1.1790043]

The equilibrium and fluctuating velocity of turbulent eddies in a magnetized plasma is a fundamental quantity characterizing the underlying turbulent-driven density fluctuations. The advent of multipoint, high-time-resolution, density fluctuation diagnostics and their turbulence imaging capability makes it feasible to directly measure such velocities and derived quantities that include the turbulent-driven particle transport, zonal flows, Reynolds Stress, and perhaps the vorticity of the turbulent fluctuating field. Several turbulence imaging diagnostics for magnetically confined plasmas have been or are being developed, including beam emission spectroscopy (BES),¹⁻³ gas puff imaging,^{4,5} and the microwave reflectometer imaging array.⁶

Methods of image-based velocimetry have been developed and utilized extensively in fluid dynamics, and application of such techniques to plasma fluctuation imaging data can provide deeper insight into turbulence phenomenon. Here, a particular velocimetry technique, orthogonal dynamic programming (ODP)⁷ is applied to beam emission spectroscopy data to ascertain the high-frequency motion of turbulent eddies, which are themselves constantly moving and morphing in the presence of the turbulent flow field. The eddy motion should itself result from fluctuations in the (radial and poloidal) $E \times B$ (electric cross magnetic field) fluctuations and therefore the underlying but unseen electrostatic fluctuations.

One-dimensional velocity fluctuations in the poloidal direction have been obtained using wavelet and other time-delay-estimation methods.⁸ These measurements exhibited clear signatures of zonal flows,^{9,10} coherent, radially localized and poloidally extended electrostatic potential structures. Here, the fluctuating velocity measurement method is extended to two dimensions.

Velocimetry techniques are applied to two-dimensional (2D) measurements of density fluctuations obtained with BES¹¹ at the DIII-D tokamak.¹² BES provides localized mea-

surements of long-wavelength ($k_{\perp} \rho_1 < 1$) density fluctuations by observing collisionally induced fluorescence of the heating neutral beams as beam atoms interact with the background plasma. Thirty two available spatial channels have been configured to obtain imaging data in a 5×6 (or 4×8 or similar) channel grid, providing a moderate spatial ($\Delta x \approx 1$ cm) and high time ($\Delta t = 1 \mu\text{s}$) resolution turbulence imaging system. BES data is typically sampled at 1 MHz, providing a continuous sequence of turbulence images for at least 0.5 s (up to 4 s with a new data acquisition system).

Velocimetry can generally be described as obtaining the spatially localized velocity flow-field of objects with a temporally resolved sequence of images. Several methods of performing velocimetry have been developed and optimized. The orthogonal dynamic programming (ODP)⁷ method is applied here as it has good spatial resolution, accuracy, and is applicable to images of amorphous structures, such as “smoke” or “bubble” images in fluid applications,¹³ or turbulent eddies in the case of plasma measurements. Other techniques have been developed and applied to particle-imaging velocimetry (PIV) such as spatial cross-correlation methods.

The technique of orthogonal dynamic programming is based on the vector-matching method of dynamic programming. The ODP method calculates a transformation that obtains a closest match between two 1D vectors. One vector is thus mapped to most closely match the other through a difference-minimization procedure. The technique is applied to 2D imaging data by decomposing the process to a sequence of 1D analyses that alternatively sample both dimensions and iteratively improve the spatial resolution, ultimately providing a 2D velocity field at the spatial resolution of the original image data. Details of the calculation are discussed in Ref. 7 and are briefly outlined here:

- (1) Each image in a temporally displaced pair (or sequence of more than two images) is subdivided into overlapping strips, or subimages, that extend across the full image in one direction, and some fraction of the image (initially half) in the perpendicular direction.

^{a)}Electronic mail: mckee@fusion.gat.com

- (2) The corresponding strips in the two (or more) images are aligned using a dynamic programming strip-to-strip matching method that enforces order and continuity. This first alignment provides an initial low-spatial resolution estimate of the velocity in the selected direction. The velocity is obtained from the distortion or mapping between strips necessary to minimize the appropriately calculated difference.
- (3) The same process is applied in the orthogonal direction, providing an initial estimate of the velocity in that direction.
- (4) The second (or later) images in the sequence are then warped or interpolated at each pixel by the initial velocity estimate, and the resulting warped images are subdivided at higher spatial resolution (narrower width), again in the two orthogonal directions (width is decreased by about $\sqrt{2}$ at each step) in sequence.
- (5) The process is repeated until the strip widths are reduced to a few pixels, providing a flow-field that is spatially resolved at the pixel resolution of the original image.

Several modifications to the basic ODP technique can further increase the accuracy and applicability of the method. These techniques include achieving subpixel resolution via interpolation during the strip matching procedure, application to multiband (e.g., color) images, and extension to multiple (>2) image sequences that experience nominally the same flow field.

To assess the accuracy of the ODP procedure and its dependence on added noise, a series of synthetic images were constructed that consist of superimposed positive and negative Gaussian-shaped “blobs.” The blobs are shifted uniformly from one image to the next [by two pixels in the “horizontal” (x) direction and one pixel in the “vertical” (y) direction] resulting in a simple, constant flow-field. The ODP algorithm accurately reproduced the expected velocity field and showed moderate to significant degradation as Gaussian noise was added to the individual frame data. The results are shown in Fig. 1, indicating the increasing uncertainty of the derived measurements with increased noise. The error bars represent the standard deviation of the resulting flow-field across the corresponding direction in the spatial and temporal data set. Above about 8–10% fractional noise level, the results degrade to an unacceptable level.

The ODP algorithm was developed to apply to two (or a few) image sequences that are obtained at relatively high spatial resolution (typically several hundred pixels in each dimension). In the case of density fluctuation images obtained with BES, the number of pixels is small, typically 5×6 , but can consist of thousands or millions of such images in a tokamak discharge sequence. The flow-field itself evolves on a time-scale of several microseconds, or a few frames. The data is also subject to significant photon (Gaussian) noise and electronic (voltage) noise from the preamplifier circuits.¹⁴ Thus, it has been necessary to slightly modify the technique for sufficiently accurate determination of the local turbulent eddy flow field. Time-series data from individual spatial channels are first frequency-filtered over the range where coherent plasma density fluctuations exist (typically over 5–250 kHz), reducing excess preamplifier and photon noise at higher frequencies, and low-frequency beam

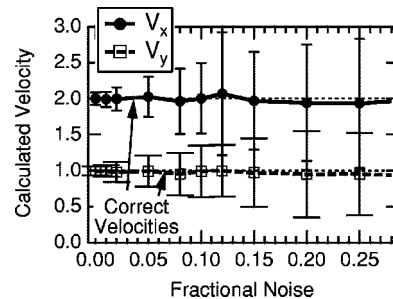


FIG. 1. Dependence of accuracy of resulting velocity field computed from orthogonal dynamic programming on applied white (Gaussian) noise to synthetic images. Dotted lines indicate actual velocity, and error bars indicate standard deviation of distribution of resulting velocity for horizontal (v_x) and vertical (v_y) velocities.

oscillations below a few kilohertz. The time-series data may also be temporally interpolated to yield a smoother image sequence for viewing. Images are then constructed at each time point by spatially interpolating the data via a 2D spline technique (resulting in a minimum curvature spline surface), effectively allowing for subpixel resolution via velocimetry analysis. The ODP algorithm is then applied simultaneously to a sequence of frames (the multiple-frame modification) to improve accuracy and reduce spurious artifacts. This multiple-frame modification allows that when the strip-to-strip matching is performed, it is performed on a summation of strips that are derived from a series of frame pairs, rather than from a single pair. This improves accuracy at the expense of time resolution. Given that the dominant underlying density fluctuations lay in range of up to a few hundred kilohertz for the data used here (relative to the 1 MHz sampling rate), the flow-field, itself derived from these fluctuations, cannot evolve on a more rapid time scale. The resulting over-sampled velocity fields are then spatially averaged to the spatial resolution of the original data set.

An example of a sequence of density fluctuation images and the resulting flow field is shown in Fig. 2. The data was acquired over an approximately 5.5×7 cm region near the outer midplane of L-mode discharge, extending across the magnetic separatrix. The images are derived from the data as described above with the derived velocity flow-field superimposed. Red represents positive density fluctuations, and blue negative fluctuations (with white near the equilibrium density). Every fourth original image is shown to illustrate the gradual evolution. Viewing movie sequences demonstrates that the evolution of the turbulent eddies is qualitatively consistent with the derived flow-field.

A quantitative test of the results is performed by examining the poloidal (vertical) motion. The flow of density fluctuations is known to have a strong poloidal (essentially vertical) component of typically several kilometers/second inside the separatrix. The time-averaged poloidal flow is measured using the established method of ensemble-averaged time-lag cross-correlation analysis.¹⁵ The time-averaged poloidal component from ODP is quantitatively compared to that obtained from cross-correlation, shown in Fig. 3. It is seen that there is a very close match between the poloidal flow derived from ODP calculations and from time-lag cross correlation. It is also interesting to note that the ODP measurements are averaged over 1 ms of data (1000

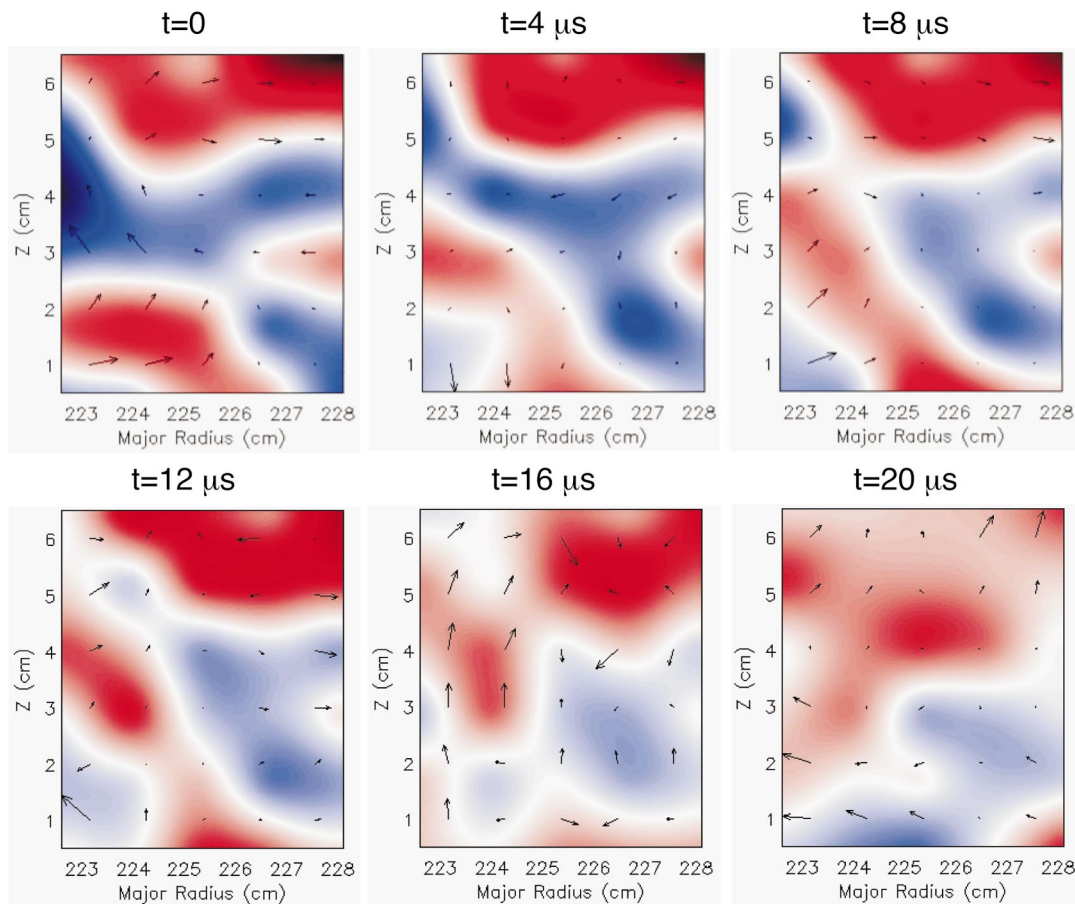


FIG. 2. (Color) Example sequence of BES density fluctuation images and superimposed velocity flow-field.

frames), while the ensemble-averaged cross-correlation measurements are averaged over 20 ms.

Future development efforts will focus on optimizing the computational efficiency and analyzing the derived flow-field to measure such critical quantities as turbulent-driven particle flux, zonal flows (including geodesic acoustic modes), the Reynolds stress, and ultimately providing an additional field of turbulent data (namely the velocity field) for use in advanced nonlinear turbulence studies. Application of these techniques to data now being acquired with a significantly higher sensitivity BES system¹⁶ should allow for turbulence velocimetry in the core regions of high-performance plasmas.

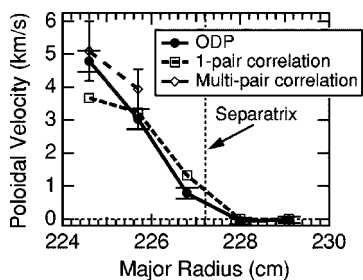


FIG. 3. Comparison of the time-averaged poloidal velocity obtained from ODP analysis to that obtained from ensemble-averaged, time-lag cross-correlation measurements (one pair indicates velocity derived from cross-correlation between two poloidally separated channels; multipair indicates velocity obtained from slope of fit to more than two channels).

This work was supported by: U.S. DOE Grant No. DE-FG03-96ER54373.

- ¹C. Fenzi, R. J. Fonck, M. Jakubowski, and G. R. McKee, *Rev. Sci. Instrum.* **72**, 988 (2001).
- ²G. R. McKee, C. Fenzi, and R. J. Fonck, *IEEE Trans. Plasma Sci.* **30**, 62 (2002).
- ³G. R. McKee, C. Fenzi, R. J. Fonck, and M. Jakubowski, *Rev. Sci. Instrum.* **74**, 2014 (2003).
- ⁴S. J. Zweben *et al.*, *Phys. Plasmas* **9**, 1981 (2002).
- ⁵R. J. Maqueda *et al.*, *Rev. Sci. Instrum.* **74**, 2020 (2003).
- ⁶T. Munsat *et al.*, *Rev. Sci. Instrum.* **74**, 1426 (2003).
- ⁷G. M. Quénot, J. Pakleza, and T. A. Kowalewski, *Exp. Fluids* **25**, 177 (1998).
- ⁸M. Jakubowski, R. J. Fonck, C. Fenzi, and G. R. McKee, *Rev. Sci. Instrum.* **72**, 996 (2001).
- ⁹M. Jakubowski, R. J. Fonck, and G. R. McKee, *Phys. Rev. Lett.* **89**, 265003 (2002).
- ¹⁰G. R. McKee *et al.*, *Phys. Plasmas* **10**, 1712 (2003).
- ¹¹G. McKee, R. Ashley, R. Durst, R. Fonck, M. Jakubowski, K. Tritz, K. Burrell, C. Greenfield, and J. Robinson, *Rev. Sci. Instrum.* **70**, 913 (1999).
- ¹²J. L. Luxon, *Nucl. Fusion* **42**, 614 (2002).
- ¹³G. M. Quénot, J. Pakleza, and T. A. Kowalewski, *Proceedings of the 8th International Symposium on Flow Visualization*, 47.1 (Sorrento, Italy 1998).
- ¹⁴R. J. Fonck, R. Ashley, R. Durst, S. F. Paul, and G. Renda, *Rev. Sci. Instrum.* **63**, 4924 (1992).
- ¹⁵R. D. Durst, R. J. Fonck, G. Cosby, and H. Evensen, *Rev. Sci. Instrum.* **63**, 4907 (1992).
- ¹⁶D. Gupta, R. J. Fonck, G. R. McKee, D. Schlossberg, and M. Shafer, *Rev. Sci. Instrum.*, these proceedings.